Lattice dynamics of II-VI materials using the adiabatic bond-charge model

B. D. Rajput and D. A. Browne
Department of Physics and Astronomy, Louisiana State University, Baton Rouge, Louisiana 70803
(Received 28 August 1995; revised manuscript received 13 December 1995)

We extend the adiabatic bond-charge model, originally developed for group IV semiconductors and III-V compounds, to study phonons in more ionic II-VI compounds with a zinc-blende structure. Phonon spectra, density of states, and specific heats are calculated for six II-VI compounds and compared with both experimental data and the results of other models. We show that the six-parameter bond-charge model gives a good description of the lattice dynamics of these materials. We also discuss trends in the parameters with respect to the ionicity and metallicity of these compounds.

I. INTRODUCTION

The adiabatic bond-charge model (BCM) has been quite successful in explaining the phonon-dispersion curves of group IV elemental semiconductors[1] and partially ionic III-V semiconducting materials[2] with a zinc-blende structure. In recent years it has been successfully applied to study phonons in semiconducting superlattices,[3,4] optical properties of $Al_xGa_{1-x}As$,[5] open semiconductor surfaces[6] and even sp^2-bonded materials like graphite[7] and fullerenes.[8] Quite recently, a modified version of the bond-charge model has been applied[9] to study the second-order Raman spectra of AlAs and AlSb.

In view of the similar dispersion curves of tetrahedrally connected III-V and II-VI materials, it is surprising that no attempt to extend BCM to the latter has appeared in the literature. This may be partly due to the comments[10] indicating that early attempts in this direction were not successful because it was found[11] that in the case of II-VI materials the asymmetry of the bond-charge position became too large to find a stable equilibrium position for the bond charges. These conclusions were based on the studies of the valence electron charge density using local pseudopotentials,[12] which suggested a nearly complete charge transfer from the cation to the anion. These calculations actually overestimated the ionicity of these compounds and produced valence band spectra in strong disagreement with experimental photoemission results.[13] Later, more accurate calculations using nonlocal pseudopotentials[14] showed better agreement with the experiments and yielded charge densities indicating a strong shift of the bond maximum rather than complete charge transfer. In fact, the charge density plots for III-V and II-VI compounds[14] are nearly identical except that the charge maxima in the latter appear to be slightly shifted toward the anion, indicating that, despite their greater ionicity, II-VI compounds are dominantly covalent in nature. In view of these results, it is expected that the BCM should give a good account of the phonons in II-VI materials provided the bond charges are placed at physically reasonable places suggested by the pseudopotential calculations.

Traditionally, the lattice dynamics of these materials has been done using rigid ion or shell models.[15–18] These models give good fits to the observed phonon-dispersion curves at the cost of a large number of adjustable parameters (10 or more), some of which have no physical interpretation. Recently, *ab initio* calculations of phonon spectra have appeared,[19] but they are are not feasible for studying large systems such as alloys like $Cd_xHg_{1-x}Te$ or thick superlattices. Therefore it is desirable to have a realistic model with fewer, physically meaningful, parameters that is easy to extend to more complex systems. In this paper we show that the six-parameter BCM provides a good description of the phonons and other lattice-dynamical quantities such as elastic constants and specific heat in II-VI materials.

The rest of the paper is organized as follows. In Sec. II we provide a brief overview of the bond-charge model.[1–3] In Sec. III we discuss the results for six II-VI compounds and in Sec. IV trends in the parameters are discussed.

II. ADIABATIC BOND-CHARGE MODEL

The adiabatic bond-charge model (BCM) for homopolar semiconductors[1] and partially ionic III-V compounds[2] is the simplest empirical lattice-dynamical model that correctly describes the phonon-dispersion curves of covalent crystals. In the BCM the valence electron charge density is represented by massless point particles, the bond charges (BC's), that follow the ionic motion adiabatically. The BCM unit cell consists of two ions and four bond charges that are placed along the bonds between the ions. In homopolar covalent crystals the bond charges are placed midway between the neighboring atoms while in III-V compounds the BC divides the bond length in the ratio of 5:3. This is consistent with nonlocal pseudopotential calculations for the valence electron charge density[14] that indicate that the charge density maximum in III-V compounds shifts toward the group V element. This shift is even stronger in the case of II-VI compounds, reflecting their more ionic character. The BCM parameter p which measures the polarity of the bond is defined in terms of the ratio in which the BC position divides the bond length. If t is the bond length and $r_1=(1+p)t/2$ and $r_2=(1-p)t/2$ are the two ion-BC distances then $p=0$ $(r_1/r_2=1)$ for homopolar materials and $p=0.25$ $(r_1/r_2=5/3)$ for III-V compounds. In our extension of the BCM to II-VI materials we have chosen to use $p=1/3$ corresponding to the ratio $r_1/r_2=2$ which is based on the results[14] of microscopic calculations. This choice will be discussed in more detail in Sec. IV.

The cation and the anion interact with one another and with the bond charges via central potentials $\phi_{ii}(t)$, $\phi_1(r_1)$, and $\phi_2(r_2)$, respectively. The bond charges centered on a common ion interact via a three-body Keating potential,[20] $V_{bb}^{\sigma}=B_{\sigma}(\vec{X}_i^{\sigma}\cdot\vec{X}_j^{\sigma}+a_{\sigma}^2)^2/8a_{\sigma}^2$, where $\vec{X}_i^{\sigma}$ is the distance vector between ion σ (σ = 1, 2) and BC i, B_{σ} is the force constant and a_{σ}^2 is the equilibrium value of $|\vec{X}_i^{\sigma}\cdot\vec{X}_j^{\sigma}|$. The bond charges centered on a particular ion also interact directly with one another through a central potential, $\psi_{\sigma}(r_{bb}^{(\sigma)})$, where $r_{bb}^{(\sigma)}$ is the distance between the bond charges centered on the cation ($\sigma=1$) or the anion ($\sigma=2$). Finally, the ions and the BC's interact via the Coulomb interaction characterized by a single parameter Z^2/ϵ where $-Ze$ is the charge of a BC, and ϵ is the dielectric constant. Each of the ions is presumed to have a charge $+2Ze$ so that the net charge in the unit cell is zero.

To reduce the number of parameters it is assumed[2] that $\psi_1'=\psi_2'=0$, $\psi_1''=-\psi_2''=(B_2-B_1)/8$ and $(1+p)\phi_1'+(1-p)\phi_2'=0$. If we use these constraints on the total lattice energy per unit cell

$$\Phi=4[\phi_{ii}(t)+\phi_1(r_1)+\phi_2(r_2)]-\alpha_M\frac{(2Z)^2}{\epsilon}\frac{e^2}{t}+6[V_{bb}^1+V_{bb}^2+\psi_1(r_{bb}^{(1)})+\psi_2(r_{bb}^{(2)})] \quad (1)$$

along with the equilibrium conditions, $\partial\Phi/\partial t=0$ and $\partial\Phi/\partial p=0$, we find[21]

$$\phi_{ii}'=-\alpha_M\frac{Z^2}{\epsilon}\frac{e^2}{t^2},$$

$$\frac{\phi_1'}{r_1}=2\frac{d\alpha_M}{dp}\frac{1-p}{1+p}\frac{Z^2}{\epsilon}\frac{e^2}{t^3},$$

$$\frac{\phi_2'}{r_2}=-2\frac{d\alpha_M}{dp}\frac{1+p}{1-p}\frac{Z^2}{\epsilon}\frac{e^2}{t^3}. \quad (2)$$

The conditions for stable equilibrium, $\partial^2\Phi/\partial t^2>0$ and $\partial^2\Phi/\partial p^2>0$, further yield

$$4\frac{\phi_{ii}''}{3}+(1+p)^2\left(\frac{\phi_1''}{3}+\frac{B_2}{6}\right)+(1-p)^2\left(\frac{\phi_2''}{3}+\frac{B_1}{6}\right)-\frac{128}{9\sqrt{3}}\alpha_M\frac{Z^2}{\epsilon}>0 \quad (3)$$

and

$$\frac{\phi_1''}{3}+\frac{\phi_2''}{3}+\frac{B_1+B_2}{24}-\frac{64}{9\sqrt{3}}\frac{d^2\alpha_M}{dp^2}\frac{Z^2}{\epsilon}>0. \quad (4)$$

The Madelung constant α_M of the model is defined by writing the Coulomb energy per unit cell as $-\alpha_M(2Ze)^2/\epsilon t$. For $p=1/3$ the values of α_M, $d\alpha_M/dp$, and $d^2\alpha_M/dp^2$ are found numerically[22] to be 5.0598, 4.0539, and 17.46, respectively. In Eqs. (3) and (4) the force constants are in units of e^2/v_a, where v_a is the unit-cell volume.

With ϕ_{ii}', ϕ_1', ϕ_2', ψ_1', ψ_2', ψ_1'', and ψ_2'' given as above, the six free parameters of the model are ϕ_{ii}'', ϕ_1'', ϕ_2'', B_1, B_2, and Z^2/ϵ, which we adjust to fit the neutron-scattering data and the measured elastic constants. The phonon eigenfrequencies and eigenvectors are found by diagonalizing the dynamical matrix[22] constructed from the BCM equations of motion

$$\mathbf{M}\omega^2\mathbf{u}=\left[\mathbf{R}+4\frac{(Ze)^2}{\epsilon}\mathbf{C}_R\right]\mathbf{u}+\left[\mathbf{T}-2\frac{(Ze)^2}{\epsilon}\mathbf{C}_T\right]\mathbf{v},$$

$$\mathbf{0}=\left[\mathbf{T}^+-2\frac{(Ze)^2}{\epsilon}\mathbf{C}_T^+\right]\mathbf{u}+\left[\mathbf{S}+\frac{(Ze)^2}{\epsilon}\mathbf{C}_S\right]\mathbf{v}. \quad (5)$$

Here $\mathbf{M}$ is the mass matrix for the ions and $\mathbf{u}$ and $\mathbf{v}$ are the vectors formed by the displacements of the ions and the BC's, respectively. The matrices $\mathbf{R}$, $\mathbf{T}$, and $\mathbf{S}$ are the dynamical matrices for the short-range ion-ion, ion-BC, and BC-BC interactions and $\mathbf{C}_R$, $\mathbf{C}_T$, and $\mathbf{C}_S$ are the corresponding Coulomb matrices which are evaluated by Ewald's method.[22] Explicit forms of $\mathbf{R}$, $\mathbf{T}$, and $\mathbf{S}$ can be found in the appendixes of Refs. 1 and 3.

III. RESULTS AND DISCUSSION

Figure 1 shows the dispersion curves for six II-VI materials along with the existing neutron-scattering data. Figure 2 shows the corresponding densities of states (DOS). We present in Table I the BCM parameters and in Table II the calculated and measured elastic constants. In all cases the overall agreement with the experimental data is fairly good and is of the same quality as for BCM fits for III-V compounds.[2] For comparison we have also included the dispersion curves for GaAs and InSb calculated using the parameters from Ref. 2. For CdTe our six-parameter fit is as good as the 14-parameter shell-model fit of Rowe *et al.*[16] and the 11-parameter rigid-ion model fit of Talwar and Vandevyer.[17] All three models show a slight upward bend in the TO branch in the (100) direction, which is in contrast with the results of a recent *ab initio* calculation.[19]

The three models give very similar predictions for the phonon density of states. The principal difference is that the shell model does not predict a gap in the DOS between the acoustic and optical contributions, while the BCM has a smaller gap than that seen in the rigid-ion model. This underscores the fact that the BCM is, in many ways, an intermediate model between the shell model and the rigid-ion model. The shell model takes care of the electronic polarizability explicitly by attaching deformable shells to the ions. The BCM partially accounts for the electronic polarizability through the adiabatic motion of the bond charges, while the rigid-ion model ignores it completely.

For ZnS and ZnTe our fits are comparable with the 10-parameter valence shell-model results of Vagelatos *et al.*[18] For ZnTe the BCM predicts a large dispersion in the LO branch near the zone edge. However, the maximum deviation from the experimentally measured frequency at the X point is only about 7%. For both ZnS and ZnTe the shape of the optical branches in the (110) direction is different from the results of Ref. 18 but is similar to that predicted[19] by *ab initio* calculations. For ZnSe also the agreement with the neutron data[23] and the measured elastic constants[24] is fairly good.

Mercury compounds, because of their semimetallic na-

ture, deserve a separate discussion. Because of the zero band gap, the energy for electronic transitions from the valence band to the conduction band is comparable to the optical-phonon energy. For HgTe Raman measurements[25] at 90 K and infrared reflectivity measurements[26] at 77 K yield $\omega_{LO} \approx 138$ cm^{-1} whereas infrared spectra at 8 K gave[27] $\omega_{LO} \approx 132$ cm^{-1}. This difference was attributed to the large number of carriers at higher temperatures. The same reason is invoked to explain the degenerate values of ω_{LO} and ω_{TO} found in neutron-scattering experiments.[28] Because of this controversy we did not use optical phonon frequencies near the zone center in our fit for HgTe. It is seen that the agreement with the acoustic- and transverse-optical phonons is good. However, the fit for the LO branch is not of the same quality, although the deviation from the experimental points is only a few percent. In the (111) direction the BCM pre-

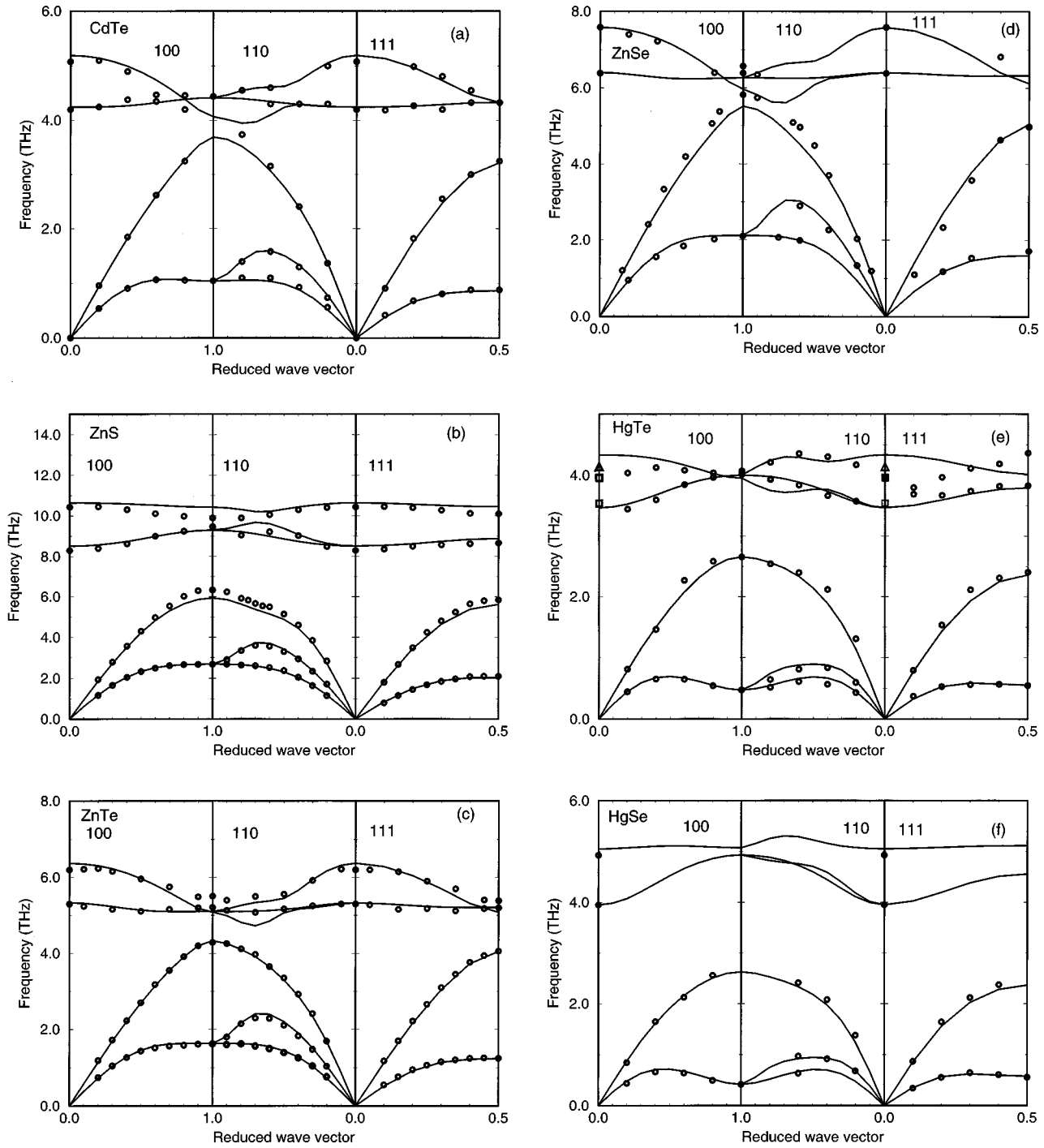

FIG. 1. Calculated phonon-dispersion curves for CdTe, ZnS, ZnTe, ZnSe, HgTe, HgSe, GaAs, and InSb. The BCM parameters for GaAs and InSb were taken from Ref. 3. Empty circles indicate neutron-scattering data taken from Refs. 16 (CdTe), 18 (ZnS and ZnTe), 23 (ZnSe), 28 (HgSe and HgTe), 39 (GaAs), and 40 (InSb). For HgTe, the open triangle is a Raman measurement of ω_{LO} from Ref. 25, and the open squares are infrared measurements of ω_{LO} and ω_{TO} from Ref. 27.

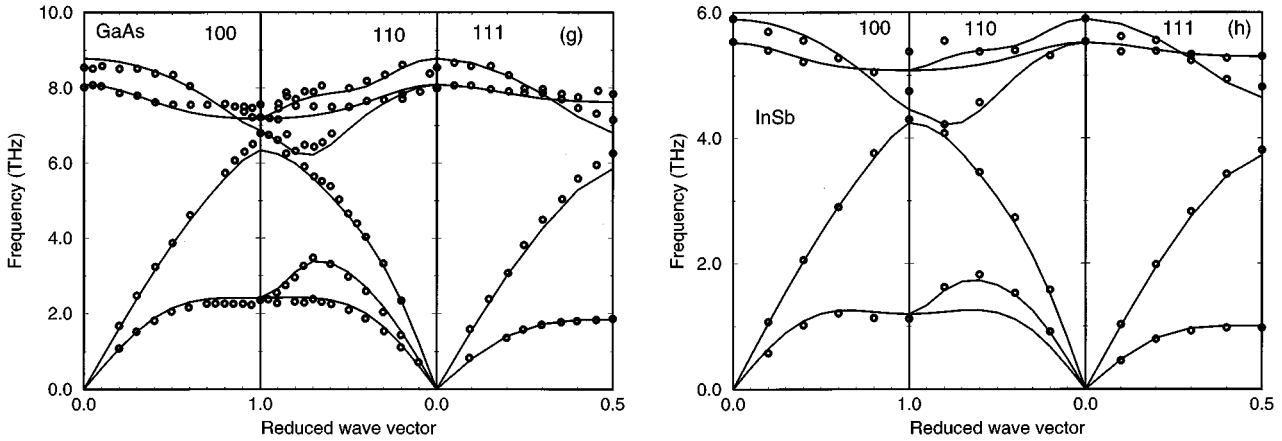

FIG. 1 (*Continued*).

dicts that the LO branch will dip downward instead of the upward trend observed experimentally.[28] For HgSe the agreement with the available neutron data on acoustic phonons[28] and optical measurements[29] and measured elastic constants[30] is very good. Because of the lack of neutron data on optical phonons we cannot comment on the accuracy of the optical branches. However, it should be mentioned that the BCM and the 11-parameter rigid-ion model[28] give similar behavior for the optical branches.

To further check the parameters we have calculated the specific heats[22] for all the six materials using the parameters given in Table I. The results are shown in Fig. 3 as plots of log$C$ vs log$T$ along with the experimental data. In every case good agreement is obtained with the experiments, giving further support for the parameters used and the calculated density of states.

A more severe test of the validity of a lattice-dynamical model is to check the eigenvectors against the experimental results. Following the convention of Refs. 31 and 32 we give, in Table III, the eigenvectors for the six II-VI materials at the X and L points of the Brillouin zone. As no information is available from experiments or from *ab initio* calculations, we cannot comment on the correctness of these vectors. However, we note that in four out of six materials, it is the lighter ion which vibrates in the higher-frequency mode (LO) at the X point. For ZnSe and CdTe, the BCM gives the opposite result and predicts that the heavier ion moves in the LO mode. This result, though counterintuitive, is not impossible since the ionic masses in these materials are comparable[33] and differences in intrasublattice forces can lead to this result. A similar pattern is obained in the case of III-V materials where the BCM predicts that at the X point the heavier ion moves in the LO mode in GaAs and InSb, which in the case of GaAs, the only relevant material whose eigenvectors have been studied experimentally,[31] is contrary to the experimental results. For materials like AlAs, GaSb, InAs, and InP, in which the mass difference is substantial, the BCM predictions agree with *ab initio* calculations.[32]

We have thus demonstrated that the six-parameter BCM provides a good description of the phonons and other lattice-dynamical quantities such as elastic constants and specific heat for II-VI compounds with zinc-blende coordination. The overall agreement with the neutron data is very good. However, some discrepancies remain, particularly in the LO branch near the zone edge, where the BCM predicts a large dispersion in almost every material including the III-V compounds. This is most obvious in HgTe and is indicative of the failure of the BCM to account for the polarizability of the ion core. Because of the associated macroscopic field, the LO phonons are more affected than the other branches. The calculated[34] static dielectric function $\epsilon(q)$ for III-V and II-VI compounds is known to have considerable structure, so including a charge form factor should remedy this discrepancy.[11]

IV. TRENDS IN PARAMETERS

Some trends in the parameters presented in Table I are immediately obvious. One notices that as one goes from group IV elements to III-V compounds to II-VI compounds the parameters involving BC's change uniformly. For group IV elements the bond charge is situated midway along the bond and the ion-BC and BC-ion-BC force constants are equal for the two ions. However, in III-V compounds the BC shifts toward the anion which results in higher values for $\phi_2''/3$ and B_2 than $\phi_1''/3$ and B_1, respectively. This trend continues as we move to II-VI compounds in which the BC is even closer to the anion. This pattern in the values of these parameters can be traced to the equations linking ϕ_1' and ϕ_2' to α_M and $d\alpha_M/dp$. It should be noted that the values for α_M and $d\alpha_M/dp$ for II-VI compounds are higher than those for III-V compounds. Apart from these obvious features, there are no other discernible trends in the parameters with respect to the ionicity or the bond length. However, it is seen that the ion-bond parameters $\phi_1''/3$ and $\phi_2''/3$ are considerably lower for mercury compounds than for other materials. This is reasonable in view of the semimetallic nature of these materials and the fact that these parameters represent off-diagonal contributions to the dielectric function.

The effect of ionicity on the phonon-dispersion curves can be investigated by studying the isoelectronic sequence of materials in which the bond lengths and the average mass in the unit cell are almost same. Two such sequences are Ge-GaAs-ZnSe and αSn-InSb-CdTe. Increased ionicity results in a general lowering of all frequencies and elastic constants

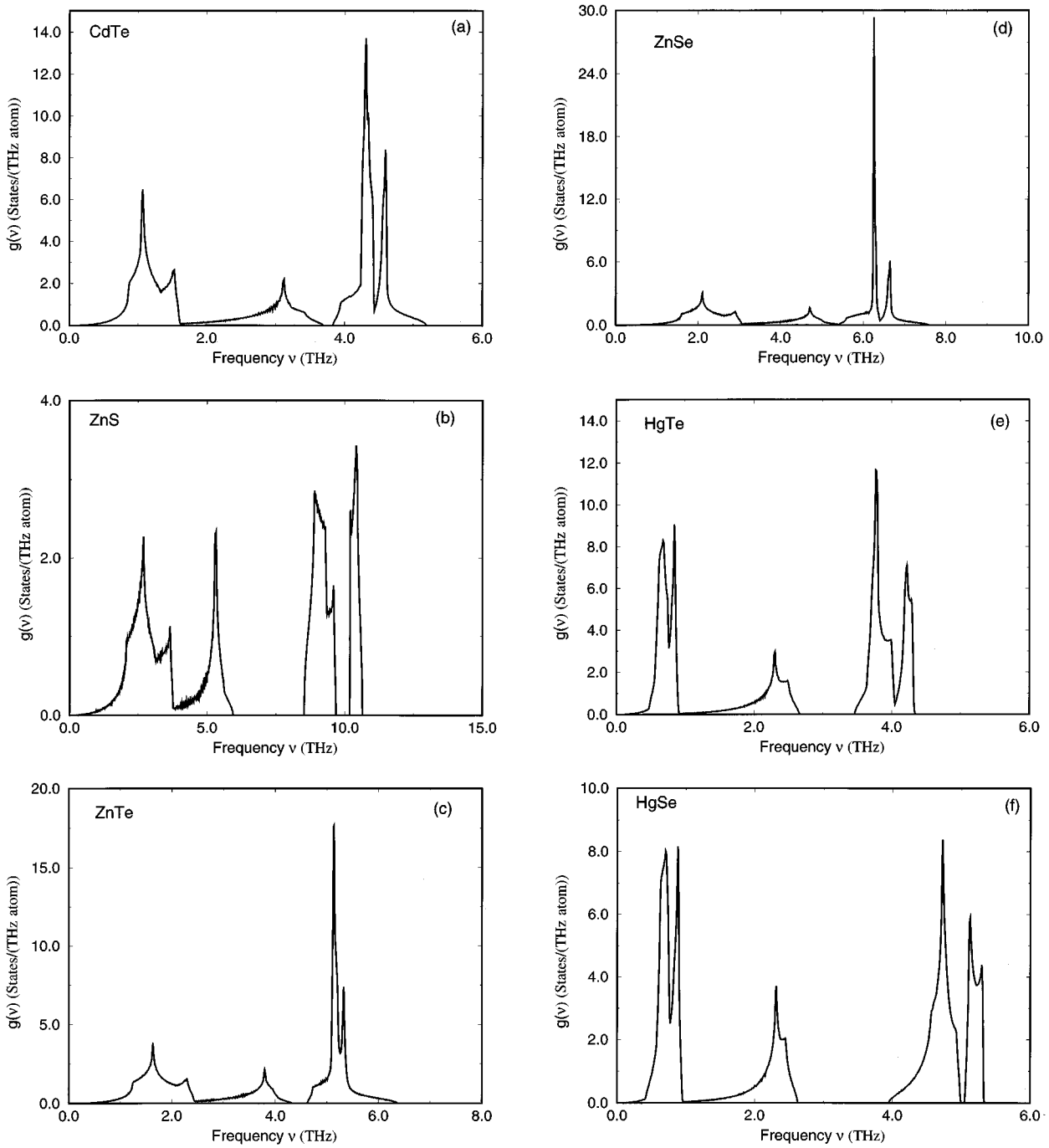

FIG. 2. Phonon density of states for II-VI compounds calculated using the root sampling method. The fine structure on the curves is an artifact of the numerical method.

and a lifting of the LO-TO degeneracy at the Γ point and the LO-LA degeneracy at the X point. A glance at the BCM parameters for these materials shows that the only pattern is a decrease in the magnitude of the bond charge Z and, in the case of Ge-GaAs-ZnSe, a decrease in $\phi''_{ii}/3$ with increased ionicity. For the other sequence, $\phi''_{ii}/3$ is almost same for α-Sn and InSb but it is smaller for CdTe. A cross comparison of the corresponding materials in the two sequences shows that moving down the periodic table, with its concomitant increase in metallicity, yields an increase in the ion-ion interaction $\phi''_{ii}/3$, while the parameters involving the bond charges decrease.

We should also comment on the choice of the equilibrium positions of the bond charges. In principle, p should be treated as the seventh adjustable parameter of the model. However, we decided to use the physically reasonable value of 1/3 for p. This corresponds to dividing the bond length in a ratio 2:1 and is consistent with the pseudopotential calculations of the valence electron charge density.[14] However, we were also able to find values for the six parameters which still satisfied the stability conditions (3) and (4) and which gave satisfactory fits for p as high as 0.55. The parameters that varied most with p were the ion-BC force constants; increasing p led to a larger $\phi''_2/3$ and a smaller $\phi''_1/3$. The

TABLE I. BCM parameters for group IV elements, III-V and II-VI compounds. Force constants are in units of e^2/v_a, where v_a is the unit-cell volume.

	$\phi''_{ii}/3$	$\phi''_1/3$	$\phi''_2/3$	B_1	B_2	Z^2/ϵ	Z [c]
Si [a]	6.21	6.47	6.47	8.60	8.60	0.1800	1.47
Ge [a]	6.61	5.71	5.71	8.40	8.40	0.1620	1.61
α-Sn [a]	7.43	5.59	5.59	7.80	7.800	0.163	1.98
AlAs [b]	5.80	2.27	15.48	5.79	8.54	0.1800	1.21
GaP [b]	6.04	2.4	17.91	5.20	10.0	0.2030	1.36
GaAs [b]	6.16	2.36	16.05	5.36	8.24	0.1870	1.43
GaSb [b]	6.77	2.37	13.10	6.28	7.08	0.1600	1.52
InP [b]	7.16	2.95	21.62	3.43	8.37	0.2490	1.55
InAs [b]	7.31	2.64	17.86	3.99	7.30	0.2100	1.60
InSb [b]	7.47	2.33	14.09	4.56	6.24	0.1720	1.64
ZnS	5.74	0.79	29.90	0.83	15.40	0.2130	1.05
ZnSe	5.01	1.19	22.82	1.21	15.65	0.1790	1.03
ZnTe	5.51	1.06	22.93	1.07	17.00	0.1800	1.05
CdTe	6.85	0.77	23.34	0.39	15.44	0.1830	1.15
HgSe	5.32	0.15	14.01	0.35	17.50	0.1095	0.91
HgTe	6.46	0.081	13.46	1.08	15.60	0.1062	1.03

[a]Parameters from Ref. 1.
[b]Parameters from Ref. 3.
[c]ϵ_∞ for HgSe from Ref. 35, for HgTe from Ref. 27 and for the rest of the materials from Ref. 36.

remaining parameters also changed, but by much less. In every case, the acoustic-phonon curves showed very good agreement with the neutron-scattering data. However, the agreement with the optical phonons slightly worsened as p increased. These results highlight the arbitrariness involved in defining the equilibrium position for the bond charges. Our choice of $p=1/3$, which coincides roughly with the position predicted by the pseudopotential calculations,[14] still gave the best overall agreement with the experimental results.

V. SUMMARY AND CONCLUSION

We have applied the adiabatic bond-charge model to study phonons in six II-VI compounds with a zinc-blende structure. The theoretical predictions of the six-parameter BCM are in good agreement with the available neutron data and the experimentally measured elastic constants and specific heats. Some minor discrepancies in the LO branch near the zone edge are believed to be due to the incomplete description of the electronic polarizability of the ions. These deviations are larger, though still only a few percent, in the case of HgTe as expected from its semimetallic nature and consequently stronger screening effects. In conclusion, we have found that the six-parameter adiabatic bond-charge model provides a satisfactory description of the lattice dynamics of tetrahedrally connected II-VI compounds. The agreement with the experimental data is of the same quality as for III-V compounds.

We have also discussed some broad trends seen in the

TABLE II. Theoretical and measured values (in parantheses) for the elastic constants in units of 10^{11} dyn/cm^2.

	c_{11}	c_{12}	c_{44}
ZnS [a]	10.907 (10.46)	6.498 (6.53)	4.678 (4.61)
ZnSe [b]	8.996 (8.59)	5.064 (5.06)	4.056 (4.06)
ZnTe [a]	7.138 (7.13)	4.233 (4.07)	3.122 (3.12)
CdTe [a]	5.675 (5.35)	4.073 (3.68)	2.047 (1.994)
HgSe [c]	6.218 (6.22)	4.647 (4.64)	2.262 (2.27)
HgTe [d]	5.631 (5.631)	3.785 (3.66)	2.123 (2.123)

[a]Measured values from Ref. 37.
[b]Measured values from Ref. 24.
[c]Measured values from Ref. 30.
[d]Measured values from Ref. 38.

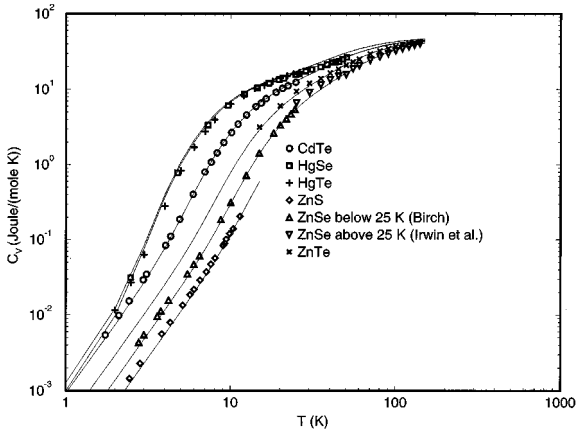

FIG. 3. log C vs log T plots for the calculated and measured specific heats of several II-VI materials. The experimental data are taken from Refs. 41–44.

TABLE III. Eigenvectors for six II-VI compounds at X and L points of the Brillouin zone. For the two degenerate transverse modes, only the magnitudes of the cationic and anionic components are given.

	ZnS	ZnSe	ZnTe	CdTe	HgSe	HgTe
$e_{\mathrm{LO}}(\mathrm{cation}\|X)$	0.0	0.0	1.0	0.0	0.0	0.0
$e_{\mathrm{LO}}(\mathrm{anion}\|X)$	1.0	1.0	0.0	1.0	1.0	1.0
$e_{\mathrm{LA}}(\mathrm{cation}\|X)$	1.0	1.0	0.0	1.0	1.0	1.0
$e_{\mathrm{LA}}(\mathrm{anion}\|X)$	0.0	0.0	1.0	0.0	0.0	0.0
$e_{\mathrm{TO}}(\mathrm{cation}\|X)$	0.260	0.636	0.815	0.611	0.252	0.400
$e_{\mathrm{TO}}(\mathrm{anion}\|X)$	0.965	0.771	0.580	0.792	0.967	0.916
$e_{\mathrm{TA}}(\mathrm{cation}\|X)$	0.876	0.826	0.812	0.823	0.834	0.824
$e_{\mathrm{TA}}(\mathrm{anion}\|X)$	0.483	0.564	0.584	0.567	0.552	0.566
$e_{\mathrm{LO}}(\mathrm{cation}\|L)$	−0.06	−0.493	0.936	−0.533	−0.125	−0.239
$e_{\mathrm{LO}}(\mathrm{anion}\|L)$	0.998	0.870	−0.351	0.846	0.992	0.971
$e_{\mathrm{LA}}(\mathrm{cation}\|L)$	0.992	0.905	0.591	0.871	0.952	0.933
$e_{\mathrm{LA}}(\mathrm{anion}\|L)$	0.121	0.425	0.807	0.491	0.305	0.361
$e_{\mathrm{TO}}(\mathrm{cation}\|L)$	0.344	0.706	0.855	0.674	0.284	0.446
$e_{\mathrm{TO}}(\mathrm{anion}\|L)$	0.939	0.708	0.519	0.738	0.959	0.895
$e_{\mathrm{TA}}(\mathrm{cation}\|L)$	0.800	0.771	0.764	0.775	0.799	0.787
$e_{\mathrm{TA}}(\mathrm{anion}\|L)$	0.599	0.637	0.611	0.632	0.601	0.615

parameters. We find that the parameters for the bond-charge-cation short-range interactions decrease with a corresponding increase in the parameters for the bond-charge-anion interactions as one goes from group IV elements to III-V to II-VI compounds.

ACKNOWLEDGMENTS

We thank T. Golding for useful conversations. This work was supported by the National Science Foundation under Grant No. NSF-DMR-9408634.

[1] W. Weber, Phys. Rev. B **15**, 4789 (1977).
[2] K. C. Rustagi and W. Weber, Solid State Commun. **18**, 673 (1976).
[3] S. K. Yip and Y. C. Chang, Phys. Rev. B **30**, 7037 (1984).
[4] L. Miglio and L. Colombo, Surf. Sci. **221**, 486 (1989).
[5] M. Bernasconi, L. Colombo, L. Miglio, and G. Benedek, Phys. Rev. B **43**, 14 447 (1991).
[6] P. Santini, L. Miglio, G. Benedek, U. Harten, P. Ruggerone, and J. P. Toennies, Phys. Rev. B **42**, 1942 (1990).
[7] G. Benedek and G. Onida, Phys. Rev. B **47**, 16 471 (1993).
[8] G. Onida and G. Benedek, Europhys. Lett. **18**, 403 (1992).
[9] T. Azuhata, T. Sota, and K. Suzuki, J. Phys. Condens. Matter **7**, 1949 (1995).
[10] K. Kunc and H. Bilz, Solid State Commun. **19**, 1027 (1976).
[11] *Encyclopedia of Physics*, edited by S. Flügge and L. Genzel (Springer-Verlag, Berlin, 1984), Vol. XXV/2d.
[12] J. P. Walter and M. L. Cohen, Phys. Rev. B **4**, 1877 (1971).
[13] D. J. Chadi, J. P. Walter, M. L. Cohen, Y. Petroff, and M. Balkanski, Phys. Rev. B **5**, 3058 (1972).
[14] J. R. Chelikowski and M. L. Cohen, Phys. Rev. B **14**, 556 (1976).
[15] K. Kunc, M. Balkanski, and M. A. Nusimovici, Phys. Status Solidi B **71**, 341 (1975).
[16] J. M. Rowe, R. M. Nicklow, D. L. Price, and K. Zanio, Phys. Rev. B **10**, 671 (1974).
[17] D. N. Talwar and M. Vandevyer, J. Appl. Phys. **56**, 1601 (1984).
[18] N. Vagelatos, D. Wehe, and J. S. King, J. Chem. Phys. **60**, 3613 (1974).
[19] A. D. Corso, S. Baroni, and R. Resta, Phys. Rev. B **47**, 3588 (1993).
[20] P. N. Keating, Phys. Rev. **145**, 637 (1966).
[21] There are a couple of misprints in Ref. 3.
[22] A. A. Maradudin, E. W. Montroll, C. H. Wiess, and I. P. Ipatova, *Theory of Lattice Dynamics in Harmonic Approximation*, 2nd ed. (Academic, New York, 1971).
[23] B. Hennion, F. Moussa, G. Pepy, and K. Kunc, Phys. Lett. **36A**, 376 (1971).
[24] B. H. Lee, J. Appl. Phys. **41**, 2988 (1970).
[25] M. L. Bansal, A. P. Roy, and A. Ingale, Phys. Rev. B **42**, 1234 (1990).
[26] J. Baars and F. Sorger, Solid State Commun. **10**, 875 (1972).
[27] M. Grynberg, R. Le Toullec, and M. Balkanski, Phys. Rev. B **9**, 517 (1974).
[28] H. Kepa, T. Giebultowicz, B. Buras, B. Lebech, and K. Clausen, Phys. Scr. **25**, 807 (1982).
[29] A. M. Witowski and M. Grynberg, Phys. Status Solidi B **100**, 389 (1980).
[30] P. J. Ford, A. J. Miller, G. A. Saunders, Y. K. Yoğurtcu, J. K. Furdyna, and M. Jaczynski, J. Phys. C **15**, 657 (1982).
[31] D. Strauch and B. Dorner, J. Phys. C **19**, 2853 (1986).
[32] P. Giannozzi, S. de Gironcoli, P. Pavone, and S. Baroni, Phys. Rev. B **43**, 7231 (1991).
[33] We have used 114 amu for the mass of Cd since the crystal in Ref. 16 was composed predominantly of the isotope ^{114}Cd.
[34] J. P. Walter and M. L. Cohen, Phys. Rev. B **2**, 1821 (1970).
[35] S. Einfeldt, F. Goschenhofer, C. R. Becker, and G. Landwehr, Phys. Rev. B **51**, 4915 (1995).
[36] K. Kunc, M. Balkanski, and M. A. Nusimovici, Phys. Status Solidi B **72**, 229 (1975).
[37] D. Berlincourt, H. Jaffe, and L. R. Shiozawa, Phys. Rev. **129**, 1009 (1963).
[38] R. I. Cottam and G. A. Saunders, J. Phys. Chem. Solids **36**, 187 (1975).
[39] J. L. T. Waugh and G. Dolling, Phys. Rev. **132**, 2410 (1963).
[40] D. L. Price, J. M. Rowe, and R. M. Nicklow, Phys. Rev. B **3**, 1268 (1971).
[41] J. C. Irwin and J. Lacombe, J. Appl. Phys. **45**, 567 (1974).
[42] J. A. Birch, J. Phys. C **8**, 2043 (1975).
[43] J. G. Collins, G. K. White, J. A. Birch, and T. F. Smith, J. Phys. C **13**, 1649 (1980).
[44] D. N. Talwar and M. Vanevyver, J. Appl. Phys. **56**, 2541 (1984).